

A New Large-Signal InP/InGaAs Single HBT Model Including Self-Heating and Impact Ionization Effects

Taeho Kim and Kyoungsoon Yang

Dept. of EECS, Korea Advanced Institute of Science and Technology (KAIST)
373-1, Guseong-dong, Yuseong-gu, Daejeon, 305-701, Republic of Korea

Abstract — A new large-signal model of InP/InGaAs single heterojunction bipolar transistors (SHBTs) has been developed which includes self-heating and impact ionization effects. The model is based on the conventional Gummel-Poon large-signal BJT model. The self-heating and impact ionization effects observed from InP-based SHBTs were modeled through a macro modeling approach. In order to take into account the dependence of impact ionization on the applied voltage and thermal effect, a feedback current source and a temperature dependent voltage source were used in the model as a function of junction temperature, I_C and V_{CB} . The model implemented in HP-ADS is verified by comparing the simulated and measured data in DC, multi-bias small-signal S-parameters and large-signal microwave power characteristics.

I. INTRODUCTION

The InP-based heterojunction bipolar transistor (HBT) has emerged as one of key technologies for micro/millimeter-wave and ultrahigh-speed applications due to inherent excellent transport-related properties [1]. One of the areas, where the InP HBT is considered to be a strong candidate among other current technologies, is the power amplifier application. Recent investigations have shown that InP-based HBTs are very promising because of their superior high-frequency as well as high-linearity performance under even low battery-voltage operation due to their low device turn-on voltage [2].

The layer structure of InP-based SHBTs uses a single heterojunction between the emitter and base (InP/InGaAs), with the base and collector both composed of InGaAs layers lattice-matched to the InP substrate. The narrow bandgap for InGaAs collector limits the breakdown voltages below 10 V, and therefore the maximum collector-emitter voltage (V_{CE}). While the low breakdown voltage of InP-based SHBTs limits the output swing voltage, output power levels up to 1.4 mW/ μm^2 at 10 GHz [3] and excellent high-linearity performance [4] have been reported. The superior high-frequency performance of InP HBTs along with high power density and linearity has led to recent active research and development for power applications under very low battery operation.

To utilize InP-based SHBTs for large-signal applications such as power amplifiers, oscillators and mixers, an accurate large-signal model is of great importance in circuit designs. Large-signal models, in which the impact ionization effect for InP-based SHBTs is accounted for, have been reported in [5], [6]. In Ref. [5], the typical soft breakdown phenomenon in InP SHBTs has been modeled by incorporating a diode breakdown model and, in Ref. [6], a polynomial current source, expressed as a function of I_C and V_{CB} , has been used. It was reported that the impact ionization in InP/InGaAs SHBTs increases with temperature [7]. However, the temperature dependence of impact ionization as well as the self-heating effect has not been taken into account in the models so far.

In this paper, we present a new large-signal InP/InGaAs single HBT model that includes both self-heating and impact ionization effects based on a macro-model approach. In Section II, the detailed procedures of developing the large-signal model are discussed. The validity of the model is verified by comparing the simulated and measured results in Section III.

II. INP/INGAAS SINGLE HBT LARGE-SIGNAL MODEL

The devices used in this study are InP/InGaAs SHBTs with an emitter size of 4-finger \times 2 \times 20 μm^2 . The devices were fabricated with a new self-aligned CDC (Crystallographically Defined emitter Contact) technology and showed peak f_T and f_{\max} of 65 GHz and 68 GHz, respectively. The detailed fabrication and layer structure have been published in [8].

The large-signal model of InP/InGaAs SHBTs, which is developed based on the conventional Gummel-Poon (G-P) large-signal BJT model, is shown in Fig. 1.

In order to take into account the soft-breakdown characteristics, which arise from the impact ionization process across the reverse biased narrow-bandgap InGaAs base-collector (B-C) junction, a feedback current source (I_{CB}) is connected externally across the B-C junction of the G-P BJT model. I_{CB} is implemented as a polynomial function of V_{CB} , I_C and junction temperature (T_j). Although the self-heating effect in InP SHBTs has not

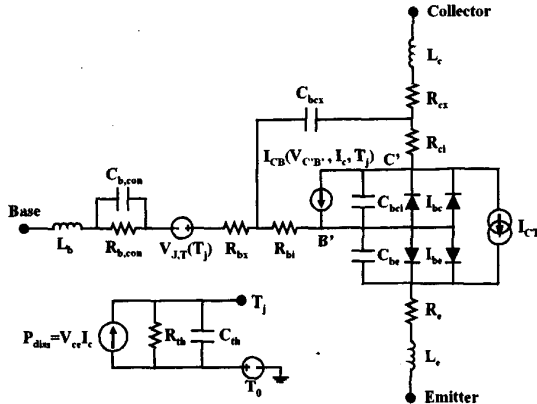


Fig. 1. Large-signal equivalent circuit model of the InP/InGaAs SHBT.

been considered in large-signal modeling so far because of rather small output voltage swing, it is found to be very important due to the low thermal conductivity of the InGaAs sub-collector layer. A thermal equivalent sub-circuit and a voltage source ($V_{i,T}$) are used to model the reduction of emitter junction built-in potential and the temperature dependence of impact ionization for the first time.

Compared to GaAs-based HBTs, which exhibit a strong dependence of DC current gain on junction temperature (T_j), InP-based HBTs demonstrate rather weak dependence on junction temperature due to the large valence-band discontinuity of InP/InGaAs (0.366 eV) [9]. So, the decrease of current gain due to self-heating is neglected in InP/InGaAs HBTs.

The DC model parameters (IS, BF, NF, ISE, NE, BR, NR, ISC, NC) of the G-P model were extracted from the measured forward and reverse Gummel plots. The parasitic resistances ($R_{b,con} + R_{bx} + R_{bi}$, R_e , $R_{ex} + R_{ci}$) and inductances (L_b , L_e , L_c) were extracted from bias-dependent S-parameter measurements under an open-collector bias condition [10]. The intrinsic capacitive parameters (CJE, VJE, MJE, CJC, VJC, MJC) were extracted from bias-dependent S-parameter measurements under different cut-off bias conditions [11].

In order to understand the contribution from the impact ionization process, the impact ionization multiplication factor ($M-1$) was extracted by measuring the device characteristics under the common-base mode with a constant I_E bias condition at different substrate temperatures [12]. The equations used for $M-1$ extraction are :

$$M-1 = \frac{\Delta I_B}{I_C(V_{CB}) - \Delta I_B}, \quad (1)$$

$$\Delta I_B = I_B(V_{CB} = 0) - I_B(V_{CB}). \quad (2)$$

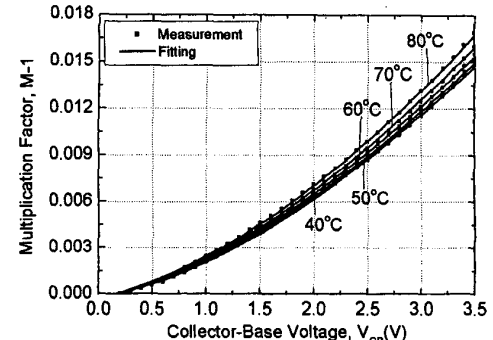


Fig. 2. Impact ionization multiplication factor (M-1) as a function of V_{CB} at different temperatures.

As shown in Fig. 2, the impact ionization multiplication factor extracted in this work increases with both the reverse bias voltage across the base-collector junction (V_{CB}) and the substrate temperature. This phenomenon is of great importance due to the possible onset of a positive feedback loop between power dissipation and impact ionization. In order to take into account this positive dependence of the impact ionization multiplication factor on V_{CB} and junction temperature in the model, the impact ionization multiplication factor was fitted using the following empirical relation with third-order polynomials of $a_i(T)$ ($i=0, 1, 2, 3$):

$$M(V_{CB}, T_j) - 1 = a_0(T_j) + a_1(T_j)V_{CB} + a_2(T_j)V_{CB}^2 + a_3(T_j)V_{CB}^3. \quad (3)$$

The measured and fitted data are shown in Fig. 2. Using the fitted M-1 [12], $I_{CB}(V_{C'B}, I_C, T_j)$ was implemented as:

$$I_{CB}(V_{CB}, I_C, T_j) = [M(V_{CB}, T_j) - 1]I_C. \quad (4)$$

The thermal-electric feedback coefficient, $-dV_{BE}/dT_j$, of the device was determined by measuring a set of forward Gummel plots at various substrate temperatures and then extracting the slopes at which the emitter junction built-in potential decreases with temperature [13]. The thermal-electric feedback coefficient was extracted by a linear fitting as:

$$-dV_{BE}/dT_i = 0.638 - 0.1733 \log_{10}(I_C) \text{ mV/}^{\circ}\text{C.} \quad (5)$$

The thermal resistance (R_{th}) was first obtained from the measured I_C - V_{CE} data at different substrate temperatures under a constant I_E bias condition [14] and then optimized. The thermal capacitance (C_{th}) was neglected in the model.

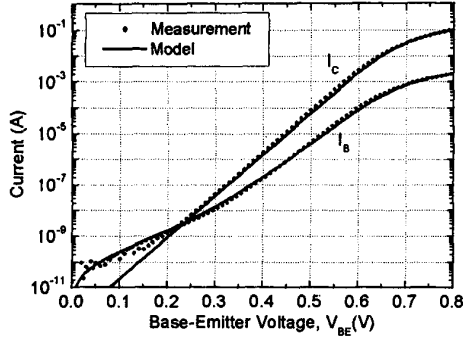


Fig. 3. Measured and modeled forward Gummel-plots.

III. SIMULATION AND MEASUREMENT

The extracted parameters for the InP/InGaAs SHBT large-signal model with an emitter size of 4-finger $\times 2 \times 20 \mu\text{m}^2$ are listed in Table I. To verify the model, the device performance in DC, multi-bias small-signal and large-signal microwave power characteristics was measured. The measured data were obtained on-wafer with an HP 4145B Semiconductor Analyzer for DC, an HP 8720C network analyzer in a frequency range of 0.5 GHz to 20 GHz for small-signal S-parameters, and a Focus microwave tuner at 10 GHz for source- and load-pull power measurements. The measurements were performed after the substrate was thinned down to 100 μm and backside gold-electroplated.

Fig. 3 shows the forward Gummel plots simulated from the developed model with the measured characteristics. The simulated and measured DC I_C - V_{CE} characteristics under the constant I_B and V_{BE} bias conditions are shown in Figures 4 and 5. The simulated data agree well with the measured data under both the constant I_B and V_{BE} bias conditions. To demonstrate the validity of the model in small-signal microwave performance, the calculated S-

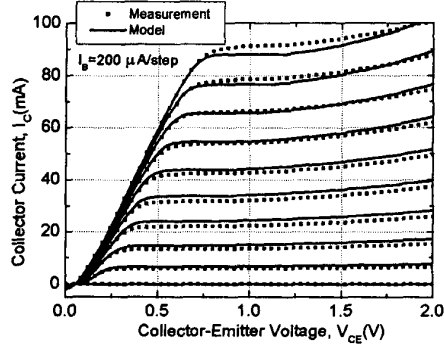


Fig. 4. Measured and modeled I_C - V_{CE} characteristics under a constant I_B bias condition.

TABLE I
EXTRACTED PARAMETERS OF THE INP/INGAAS SHBT

Parameter	Value	Parameter	Value
IS	$6.8 \times 10^{-13} \text{ A}$	TF	0.87 ps
BF	1000	XTF	0.901638
NF	1.05	VTF	1.517 V
VAF	∞	ITF	0.3 mA
IKF	∞	EG	0.75 eV
ISE	$9.0 \times 10^{-13} \text{ A}$	R_{bi}	1.01271 Ω
NE	1.258	R_{bx}	1.0 Ω
BR	0.75	R_e	1.0 Ω
NR	1.0265	R_{ci}	2.5 Ω
VAR	∞	R_{cx}	2.0 Ω
IKR	∞	$R_{b,con}$	10.42455 Ω
ISC	$2.2068 \times 10^{-11} \text{ A}$	$C_{b,con}$	1.83 pF
NC	1.20336	L_b	54.48 pH
IRB	∞	L_c	28.032 pH
RBM	0 Ω	L_e	14.2 pH
CJE	305.173 fF	C_{pbe}	35 fF
VJE	1.44359 V	C_{pbc}	1.0 fF
MJE	0.942	C_{pce}	40 fF
CJC	450.421 fF	C_{bcx}	17 fF
VJC	0.556571 V	R_{th}	500 $^{\circ}\text{C/W}$
MJC	0.9422		

parameters using the model are compared with the experimental results at two different bias points in Fig. 6. In the figure, reasonably good agreement is shown between the simulated and measured S-parameters. Fig. 7 shows the measured and simulated large-signal microwave power characteristics at a frequency of 10 GHz. The power measurement was conducted by optimizing the source and load impedances for maximum output power ($\Gamma_{\text{Source}}=0.418 \angle 180.1^{\circ}$, $\Gamma_{\text{Load}}=0.638 \angle 187.3^{\circ}$). As shown in Fig. 7, the simulated data using the developed model agree well with the measured data.

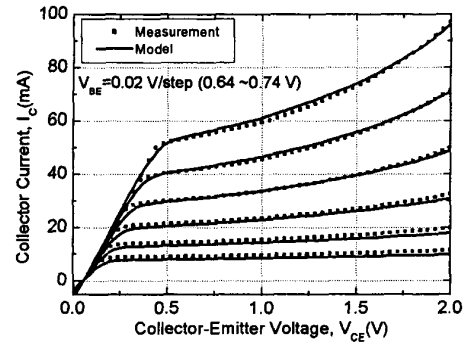


Fig. 5. Measured and modeled I_C - V_{CE} characteristics under a constant V_{BE} bias condition.

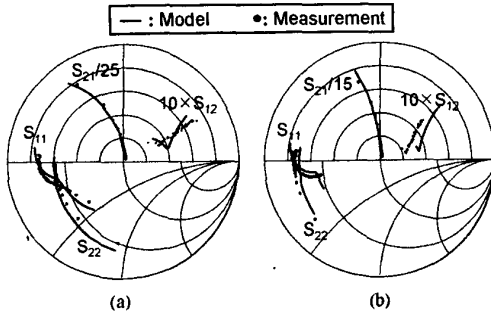


Fig. 6. Measured and modeled S-parameters from 0.5 GHz to 20 GHz for bias operating conditions of (a) $I_B=1.0$ mA, $V_{CE}=1.25$ V and (b) $I_B=1.8$ mA, $V_{CE}=1.0$ V.

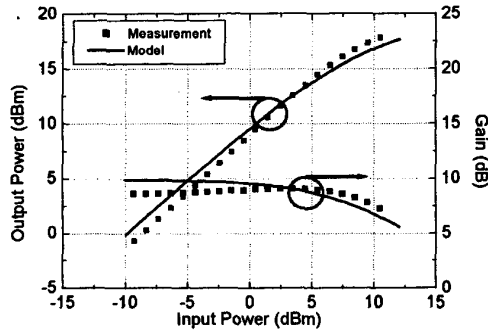


Fig. 7. Measured and modeled microwave power characteristics at 10 GHz for a bias condition of $V_{BE}=0.7$ V and $V_{CE}=2.0$ V ($\Gamma_{Source}=0.418\angle 180.1^\circ$, $\Gamma_{Load}=0.638\angle 187.3^\circ$).

IV. CONCLUSION

A new large-signal InP/InGaAs SHBT model has been developed and implemented in HP-ADS, which can account for the self-heating and impact ionization effects. The impact ionization effect has been successfully modeled using a feedback current source which is implemented as a function of V_{CB} , I_c and junction temperature. Good agreement between the measured and simulated data using the developed model has been achieved in the overall device performance of DC, multi-bias small-signal and large-signal microwave power characteristics.

ACKNOWLEDGEMENT

The authors would like to thank Prof. Songcheol Hong and Hyun-Min Park for helpful discussions. This work was supported by the National Program for Tera-level Nanodevices.

REFERENCES

- [1] K. W. Kobayashi, and et al., "A 0.5 Watt-40 % PAE InP Double Heterojunction Bipolar Transistor K-band MMIC power amplifier," *Proc. 12th Int. Conf. Indium Phosphide and Related Materials*, pp. 250-253, May 2000.
- [2] D. C. Streit, and et al., "Production and commercial insertion of InP HBT Integrated circuits," *19th Annu. GaAs IC Symp. Dig.*, pp. 135-138, Oct. 1997.
- [3] D. Sawdai, and et al., "Power performance of InGaAs/InP single HBTs," *Proc. 8th Int. Conf. Indium Phosphide and Related Materials*, pp. 133-136, Apr. 1996.
- [4] L. W. Yang, and et al., "High linearity K-band InP HBT power amplifier MMIC with 62.8% PAE at 21 GHz," *19th Annu. GaAs IC Symp. Dig.*, pp. 73-76, Oct. 1999.
- [5] A. Samelis, D. Pavlidis, S. Chandrasekhar, L. M. Lunardi and J. Rios, "Large-signal characteristics of InP-based HBTs and optoelectric cascode transimpedance amplifiers," *IEEE Trans. Electron Devices*, vol. 43, no. 12, pp. 2053-2061, Dec. 1996.
- [6] K. Yang, A. L. Gutierrez-Aitken, X. Zhang, P. Battacharya and G. I. Haddad, "An HSPICE HBT model for InP-based single HBTs," *IEEE Trans. Electron Devices*, vol. 43, no. 9, pp. 1470-1472, Sept. 1996.
- [7] D. Ritter, R. A. Hamm, A. Feygenson and M. B. Ranish, "Anomalous electric field and temperature dependence of collector multiplication in InP/Ga_{0.47}In_{0.53}As HBTs," *Applied Physics Letters*, vol. 60, no. 25, pp. 3150-3152, June 1992.
- [8] M. Kim, T. Kim, S. Jeon, M. Yoon, Y. S. Kwon and K. Yang, "Performance of new self-aligned InP/InGaAs HBTs using crystallographically defined emitter contact technology," *Proc. 13th Int. Conf. Indium Phosphide and Related Materials*, pp. 220-223, May 2001.
- [9] W. Liu, S. K. Fan, T. Henderson and D. Davito, "Temperature dependence of current gain in GaInP/GaAs and AlGaAs/GaAs HBTs," *IEEE Trans. Electron Devices*, vol. 40, no. 7, pp. 1351-1353, July 1993.
- [10] C.-J. Wei and J. C. M. Hwang, "Direct extraction of equivalent circuit parameters for HBTs," *IEEE Trans. Microwave Theory and Tech.*, vol. 43, no. 9, pp. 2035-2040, Sept. 1995.
- [11] B. Li, S. Prasad, L.-W. Yang and S. C. Wang, "A semianalytical parameter-extraction procedure for HBT equivalent circuit," *IEEE Trans. Microwave Theory and Tech.*, vol. 46, no. 10, pp. 1427-1435, Oct. 1998.
- [12] A. Neviani, G. Meneghesso, E. Zanoni, M. Hafizi and C. Canali, "Positive temperature dependence of the electron impact ionization coefficient in In_{0.53}Ga_{0.47}As/InP HBTs," *IEEE Electron Device Letters*, vol. 18, no. 12, pp. 619-621, Dec. 1997.
- [13] W. Liu, "Thermal management to avoid the collapse of current gain in power HBTs," *IEEE GaAs IC Symp.*, pp. 147-150, 1995.
- [14] D. E. Dawson, A. K. Gupta and M. L. Salib, "CW measurement of HBT thermal resistance," *IEEE Trans. Electron Devices*, vol. 39, no. 10, Oct. 1992.